

# RSC Advances



This is an *Accepted Manuscript*, which has been through the Royal Society of Chemistry peer review process and has been accepted for publication.

*Accepted Manuscripts* are published online shortly after acceptance, before technical editing, formatting and proof reading. Using this free service, authors can make their results available to the community, in citable form, before we publish the edited article. This *Accepted Manuscript* will be replaced by the edited, formatted and paginated article as soon as this is available.

You can find more information about *Accepted Manuscripts* in the [Information for Authors](#).

Please note that technical editing may introduce minor changes to the text and/or graphics, which may alter content. The journal's standard [Terms & Conditions](#) and the [Ethical guidelines](#) still apply. In no event shall the Royal Society of Chemistry be held responsible for any errors or omissions in this *Accepted Manuscript* or any consequences arising from the use of any information it contains.

Cite this: DOI: 10.1039/c0xx00000x

www.rsc.org/xxxxxx

ARTICLE TYPE

# Water-dispersible and Magnetic Separable Gold Nanoparticles Supported on Magnetite/S-Graphene nanocomposite and their Catalytic Application in Ullmann coupling of aryl iodides in Aqueous Media

Minoo Dabiri,<sup>a\*</sup> Monire Shariatipour,<sup>a</sup> Siyavash Kazemi Movahed,<sup>a</sup> and Sahareh Bashiribod<sup>b</sup><sup>5</sup> Received (in XXX, XXX) Xth XXXXXXXXX 20XX, Accepted Xth XXXXXXXXX 20XX

DOI: 10.1039/b000000x

The water-dispersible sulfonated graphene (s-G) was synthesized by anchoring the sulfonic acid groups on graphene sheets. Subsequently, the magnetic separable Fe<sub>3</sub>O<sub>4</sub>/s-G was synthesized from the Fe<sub>3</sub>O<sub>4</sub> nanoparticles decorated on s-G sheets by the co-precipitation method of iron ions. Finally, Fe<sub>3</sub>O<sub>4</sub>/s-G was successfully decorated with gold nanoparticles in a facile route by reducing chloroauric acid in the presence of sodium dodecyl sulfate, which is used as both a surfactant and reducing agent. The obtained Au/Fe<sub>3</sub>O<sub>4</sub>/s-G nanocomposite remained soluble in water, but could be easily separated from reaction solutions by an external magnetic field and then used as a heterogeneous catalyst for the Ullmann coupling reaction in water. The catalytic activity reduction was not significant even after five consecutive reaction runs due to the efficient magnetic separation, the high dispersion and stability of the catalyst in aqueous solution.

## 15 Introduction

Noble metal nanoparticles such as Au, Pd, Ru, Rh have aroused considerable attention in a wide variety of applications due to their unique physicochemical properties, especially their catalytic activity in a number of chemical reactions.<sup>1</sup> To enhance their stability and catalytic activity, they are often deposited onto supporting materials forming catalytic systems.<sup>2</sup> Recent years witness a tremendous growth in the number of supported gold nanoparticles (Au NPs) catalysing highly selective chemical transformations.<sup>3</sup> The catalytic performance of Au NPs-support strongly depends on the size and shape of Au NPs, the nature of the support, and the Au NPs-support interface interaction.<sup>4</sup> Supporting carriers may function by dispersing and fixing the Au NPs. Supports such as oxides and mixed oxides (CeO<sub>2</sub>,<sup>5</sup> SiO<sub>2</sub>,<sup>6</sup> Al<sub>2</sub>O<sub>3</sub>,<sup>7</sup> TiO<sub>2</sub>,<sup>8</sup> Mg–Al–O<sup>9</sup> and Ga–Al–O<sup>10</sup>), polymers (PVP<sup>11</sup> and PS Derivatives<sup>12</sup>) and ordered mesoporous carbon<sup>13</sup> have been used for supporting Au NPs. Among these,  $\pi$ -interaction of aromatic rings with gold nanoparticles leads to nanoparticle stabilization and improve the catalyst performance in a variety of gold-catalyzed reactions.<sup>4,12,14</sup> Graphene is an ideal candidate because of its a two-dimensional sheet of sp<sup>2</sup> bonded carbon atoms, which can be viewed as an extra-large polycyclic aromatic molecule and large specific surface area.<sup>15</sup> Loading metal NPs onto graphene can not only prevent graphene sheets from restacking but also improve the catalytic performance owing to the strong synergistic interaction between the two components.<sup>16</sup> Therefore graphene as a polycyclic aromatic molecule is a potential candidate as both support and stabilizer of Au NPs for chemical transformations.

Recently, much attention has been paid on the synthesis of Fe<sub>3</sub>O<sub>4</sub> NPs/graphene as a new kind of hybrid material, owing to wide-ranging applications such as immobilizing bioactive substances, energy storage and environmental remediation.<sup>16,17</sup>

The unique properties of Fe<sub>3</sub>O<sub>4</sub> NPs/graphene hybrids, combining characteristics of graphene as a polycyclic aromatic molecule, which has high conductivity, low price, high chemical inertness, and large specific surface area,<sup>15</sup> and Fe<sub>3</sub>O<sub>4</sub> NPs, with high magnetism, low expense, and environmentally benign nature,<sup>18</sup> open a new window for fabricating highly stable multifunctional nanomaterials using these hybrids as support materials. In addition, Fe<sub>3</sub>O<sub>4</sub> has already been introduced as a suitable support for preparing highly active metal catalysts, and immobilizing noble metal nanocatalysts on magnetic Fe<sub>3</sub>O<sub>4</sub> support prevents agglomeration of the catalyst particles during recovery and can increase catalyst durability.<sup>19</sup> Thus, a combination of Fe<sub>3</sub>O<sub>4</sub> NPs and graphene may optimize both dispersion and catalytic activity of metal NPs.

However, due to the weak dispersity of graphene in water and organic solvents, it is difficult to graft foreign nanostructures (such as NPs) on the graphene surface. In order to enhance the dispersity of graphene for facilitating the subsequent functionalization, various functionalized graphene sheets were synthesized. It is well-known that the s-G is water dispersible without the need for any polymeric or surfactant stabilizers. The negatively charged SO<sub>3</sub><sup>-</sup> units prevent the graphitic sheets from aggregating in solution thereby yielding isolated sheets of s-G with improved water dispersity.<sup>20</sup>

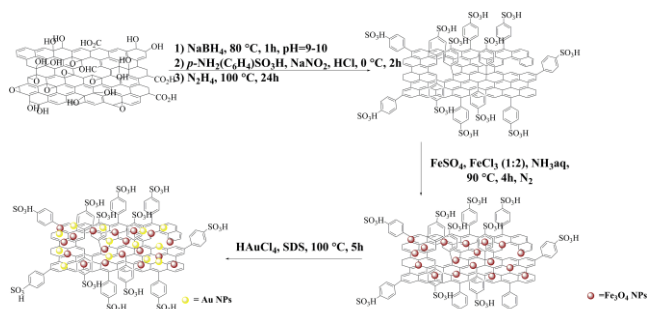
Aryl–aryl bond formation reactions are one of the most important reactions in organic synthesis as they give rise to many naturally occurring biologically and pharmaceutically active products. The original and most widely used route to produce biaryls is *via* the Ullmann reaction, the copper-mediated homo-coupling of aryl halides. The need to avoid the harsh conditions typically required for Ullmann couplings (>140 °C, stoichiometric amounts of copper and selective halide substrates) have motivated researchers to find milder variations. Although, significant progress in this area has been achieved with a variety

of Pd, Cu, and Ni-based catalysts, the majority of reports about Ullmann protocols are still homogeneous and successful examples using heterogeneous and recyclable catalyst systems are limited.<sup>21</sup> However, only a few studies have involved the application of free or supported Au NPs as catalyst in Ullmann type reaction of aryl iodides.<sup>22-24</sup> Furthermore, literature reports involving homocoupling of aryl iodides catalysed by Au NPs in water are very scarce.<sup>25</sup>

Herein, we report a novel and easy approach to homogeneously immobilize Fe<sub>3</sub>O<sub>4</sub> and Au nanoparticles on sulfonated graphene sheets (s-G). The catalyst is designed with the aim of combining the excellent supporting property of graphene effectively immobilizing and stabilizing Fe<sub>3</sub>O<sub>4</sub> and Au nanoparticles with the magnetic property of the Fe<sub>3</sub>O<sub>4</sub> nanoparticles for easy separation of catalyst and therefore improving their reusability. Additionally, this nanocomposite is shown to act as an efficient heterogeneous catalyst for the Ullmann homocoupling reaction in aqueous solution under aerobic condition and could be efficiently reused while keeping the inherent catalytic activity.

## Results and Discussion

The process for the preparation of Au/Fe<sub>3</sub>O<sub>4</sub>/s-G nanocomposite is schematically described in Scheme 1. The s-G nanocomposite was synthesized by Samulski method.<sup>20</sup> Subsequently, the magnetic separable Fe<sub>3</sub>O<sub>4</sub>/s-G was synthesized from the Fe<sub>3</sub>O<sub>4</sub> nanoparticles decorated on s-G sheets by the co-precipitation method of FeSO<sub>4</sub> and FeCl<sub>3</sub> as iron ions in pH=8-9.<sup>26</sup> Finally, Fe<sub>3</sub>O<sub>4</sub>/s-G was successfully decorated with gold nanoparticles in a facile route by reducing chloroauric acid (HAuCl<sub>4</sub>) in the presence of sodium dodecyl sulfate (SDS), which is used as both a surfactant and reducing agent.<sup>27</sup>



**Scheme 1** Schematic illustration of the preparation procedure of Au/Fe<sub>3</sub>O<sub>4</sub>/s-G nanocomposite

Raman spectroscopy is a very useful tool for investigating the electronic and phonon structure graphene-based materials.<sup>28</sup> The Raman spectra of the prepared s-G, Fe<sub>3</sub>O<sub>4</sub>/s-G and Au/Fe<sub>3</sub>O<sub>4</sub>/s-G are shown in Fig. 1. The characteristic D and G bands of carbon materials were observed around 1301 and 1386 cm<sup>-1</sup>, respectively in Raman spectrum of s-G (Fig. 1). The D band is characteristic of a breathing mode for *k*-point phonons of A<sub>1g</sub>, while the G band is the result of the first-order scattering of the E<sub>2g</sub> mode of sp<sup>2</sup> carbon domains.<sup>29</sup> The Raman spectrum of Fe<sub>3</sub>O<sub>4</sub>/s-G composite displays signals at 200-700 cm<sup>-1</sup>, which are due to the Fe<sub>3</sub>O<sub>4</sub> NPs, and slightly split signal centred at 1293 cm<sup>-1</sup>, which represents the overlap of two peaks, one from Fe<sub>3</sub>O<sub>4</sub> at 1280 cm<sup>-1</sup> and a

typical graphene D band peak at 1301 cm<sup>-1</sup>.<sup>30</sup> Another typical graphene signal is also observed at 1573 cm<sup>-1</sup>, which is identified as the G band of graphene. The Raman spectrum of Au/Fe<sub>3</sub>O<sub>4</sub>/s-G shows signals of Fe<sub>3</sub>O<sub>4</sub> NPs and graphene. Additionally, after conjugation of the Au NPs onto the Fe<sub>3</sub>O<sub>4</sub>/s-G sheets, the intensity of the Raman signals of graphene (D and G bands) were enhanced relative to Fe<sub>3</sub>O<sub>4</sub>/s-G, because of the surface enhanced Raman spectroscopy (SERS) of Au NPs. SERS were obtained *via* an electromagnetic enhancement (excitation of localized surface plasmons involving a physical interaction) or chemical enhancement (formation of charge-transfer complexes involving chemical interaction) with enhancement factors of ~10<sup>12</sup> and ~10 to 100, respectively. The low enhancement factor for the Au/Fe<sub>3</sub>O<sub>4</sub>/s-G nanocomposite indicates the presence of a chemical interaction or bonding between Au NPs and Fe<sub>3</sub>O<sub>4</sub>/s-G.<sup>31</sup> The enhanced broad peak in the frequency region of 400–800 cm<sup>-1</sup> is due to the amorphous sp<sup>3</sup> bonded carbon in Au/Fe<sub>3</sub>O<sub>4</sub>/s-G nanocomposite.<sup>32</sup> To be assured, we synthesized a sample without magnetic nanoparticles (Au/s-G) and the similar peak was observed in this area (Fig. S1).

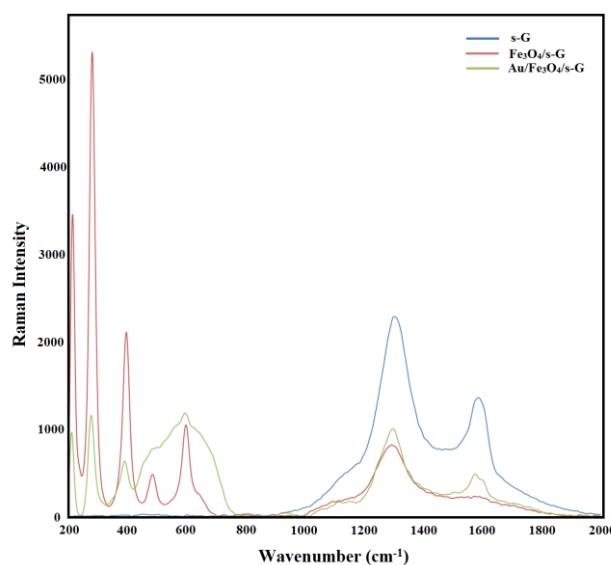


**Fig. 1** Raman spectra of s-G, Fe<sub>3</sub>O<sub>4</sub>/s-G and Au/Fe<sub>3</sub>O<sub>4</sub>/s-G nanocomposites

The electronic properties of Au/Fe<sub>3</sub>O<sub>4</sub>/s-G nanocomposite was probed by X-ray photoelectron spectroscopy (XPS) analysis. As shown in Fig. 2a, the peaks corresponding to Au 4d & 4f, C 1s, Fe 2p & 2s, O 1s, and S 2p & 2s are clearly observed in the XPS full spectrum. The S 2p spectrum of Au/Fe<sub>3</sub>O<sub>4</sub>/s-G nanocomposite is shown in Fig. 2b. The S 2p signal for Au/Fe<sub>3</sub>O<sub>4</sub>/s-G nanocomposite includes two components. The first one is constituted by two doublets, situated at 166.54 and 168.13 eV, respectively, attributable to SO<sub>3</sub>H groups on s-G sheets.<sup>33</sup> The second component located at 169.52 and 171.88 eV is attributable to the sulfur atoms of the dodecyl sulfate anions as surfactant of Au NPs.<sup>34</sup> From the Fe 2p XPS scan shown in Fig. 2c, the two peaks at 726.28 and 711.99 eV, are assignable to Fe 2p<sub>1/2</sub> and Fe 2p<sub>3/2</sub> for Fe<sub>3</sub>O<sub>4</sub>, respectively.<sup>35</sup> The XPS spectrum of Au 4f core for Au NPs-RGO level displays main peaks at 83.79 and 87.56 eV which correspond to the binding energy of Au<sup>0</sup> 4f<sub>7/2</sub> and Au<sup>0</sup> 4f<sub>5/2</sub>, respectively (Fig. 2d).<sup>36</sup>

Fig. 3a depicts the scanning electron microscope (SEM) micrograph of Au/Fe<sub>3</sub>O<sub>4</sub>/s-G sample. Several graphene layers and folds in their planes are visible. The density and distribution of elements of the Au, Fe, and S on the Au/Fe<sub>3</sub>O<sub>4</sub>/s-G nanocomposite are evaluated by quantitative energy dispersive X-ray spectroscopy (EDS) mapping. As is seen in Fig. 4b-d, rather than only located at the edges of s-G sheets, the elements Au, Fe, and S are found to be uniformly dispersed on the whole surface of Au/Fe<sub>3</sub>O<sub>4</sub>/s-G nanocomposite.

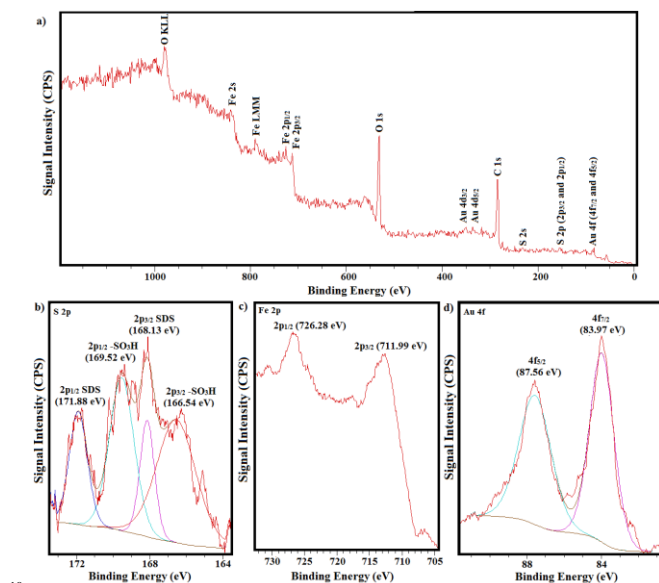


**Fig. 2** a) Full range XPS spectrum of Au/Fe<sub>3</sub>O<sub>4</sub>/s-G nanocomposite. b) S 2p, c) Fe 2p, and d) Au 4f core level regions XPS spectra of Au/Fe<sub>3</sub>O<sub>4</sub>/s-G nanocomposite, respectively.

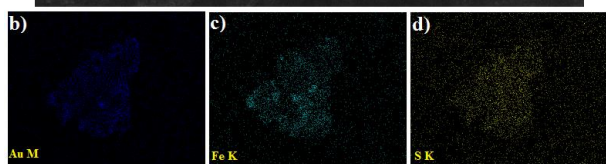
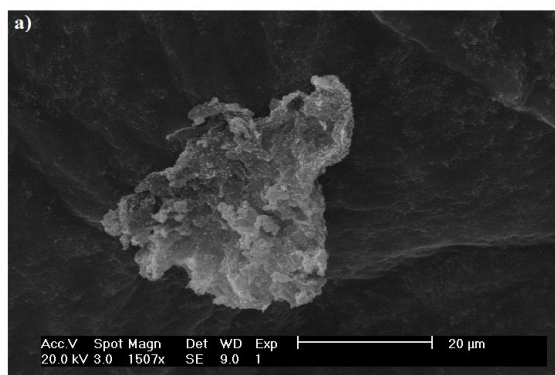


**Fig. 3** Scanning electron micrograph of a) Au/Fe<sub>3</sub>O<sub>4</sub>/s-G nanocomposite and corresponding quantitative EDS element mapping of b) Au, c) Fe and d) S.

Fig. 4a and 4c show a comparison between the morphologies of Fe<sub>3</sub>O<sub>4</sub>/s-G, and Au/Fe<sub>3</sub>O<sub>4</sub>/s-G nanocomposites investigated using transmission electron microscope (TEM). As Fig. 5a shows, the surfaces of s-G are covered with good dispersion of Fe<sub>3</sub>O<sub>4</sub> NPs with an average size of 10–20 nm. Fig. 4b. shows

selected area electron diffraction (SAED) pattern of Fe<sub>3</sub>O<sub>4</sub>/s-G nanocomposite. Fig. 4c-e shows the large-sized particles and no agglomeration of Au NPs in Fe<sub>3</sub>O<sub>4</sub>/s-G sheets. Fig. 4f shows SAED pattern of Au/Fe<sub>3</sub>O<sub>4</sub>/s-G nanocomposite. Additionally, Au and Fe<sub>3</sub>O<sub>4</sub> NPs are not found outside of the s-G sheets.

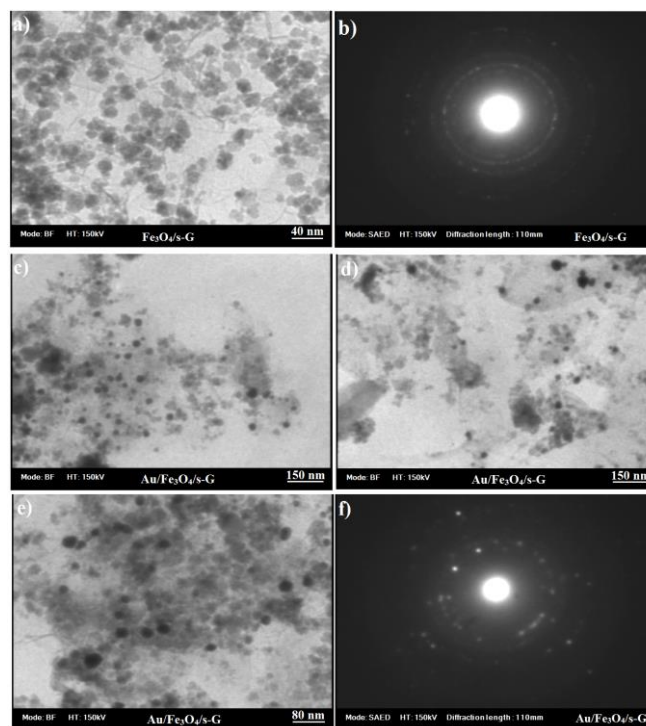


**Fig. 4** a) TEM of Fe<sub>3</sub>O<sub>4</sub>/s-G nanocomposite b) SEAD pattern of Fe<sub>3</sub>O<sub>4</sub>/s-G nanocomposite, c-e) TEM of Au/Fe<sub>3</sub>O<sub>4</sub>/s-G nanocomposite and f) SEAD pattern of Au/Fe<sub>3</sub>O<sub>4</sub>/s-G nanocomposite

As shown in Fig. 5a the Au/Fe<sub>3</sub>O<sub>4</sub>/s-G nanocomposite provide a homogeneous and stable suspension after dispersing in water due to the presence of SO<sub>3</sub>H groups in its surface. Moreover, the strong magnetic property of the prepared nanocomposite was revealed by complete and easy attraction by an external magnet field (Fig. 5b).

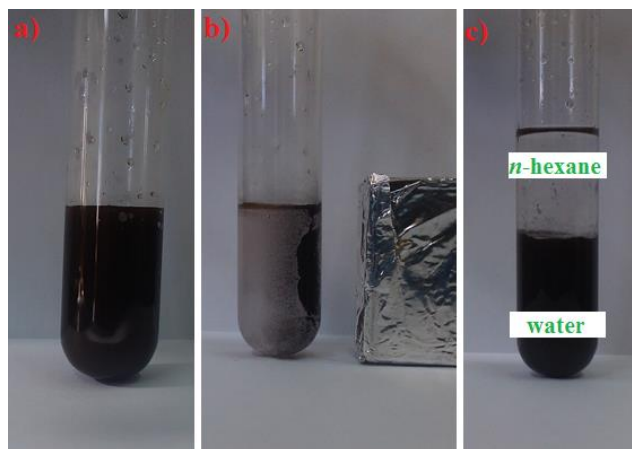


**Fig. 5** The digital images of a) water soluble Au/Fe<sub>3</sub>O<sub>4</sub>/s-G nanocomposite, b) easy separation of Au/Fe<sub>3</sub>O<sub>4</sub>/s-G nanocomposite by an external magnet field, and c) distribution of Au/Fe<sub>3</sub>O<sub>4</sub>/s-G nanocomposite in a biphasic water/n-hexane system



The magnetic properties of Au/Fe<sub>3</sub>O<sub>4</sub>/s-G nanocomposite was investigated by a vibrating sample magnetometer (VSM) at room temperature in external magnetic fields ranging from -8000 to 8000 Oe. As illustrated in Fig. 6, the magnetization curve of the prepared material has little hysteresis, remanence, and coercivity, which demonstrates their superparamagnetic characteristics.<sup>16</sup> The saturation magnetization of the Au/Fe<sub>3</sub>O<sub>4</sub>/s-G nanocomposite was found to be 10.06 emu g<sup>-1</sup> as measured. This value is smaller than the reported value of Fe<sub>3</sub>O<sub>4</sub> bulk of 92 emu g<sup>-1</sup>.<sup>37</sup> This could be attributed to the presence of magnetically inactive layers at nanoparticle surfaces. This effect becomes more pronounced as particle size decreases.<sup>38</sup> Additionally, the relatively low amount of Fe<sub>3</sub>O<sub>4</sub> loaded on S-G, which is estimated to be 15.23 wt% calculated from the content of Fe by inductively coupled plasma-optical emission spectrometry (ICP-OES).

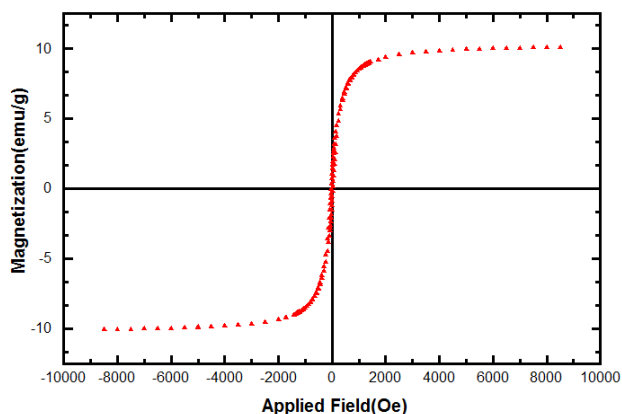


Fig. 6 The VSM curve of Au/Fe<sub>3</sub>O<sub>4</sub>/s-G nanocomposite.

The catalytic activity of Au/Fe<sub>3</sub>O<sub>4</sub>/s-G nanocomposite was then tested in the Ullmann coupling reaction. We chose the homocoupling phenyl iodide as a model reaction in H<sub>2</sub>O as solvent at 110 °C in the presence of K<sub>2</sub>CO<sub>3</sub> as base and with a catalyst loading of 2 mol% of Au. Under these conditions, we found that the cross coupling reaction proceeds well, affording the promising low yields (27%) of the corresponding biphenyl (Table 1, entry 1). Various bases such as K<sub>3</sub>PO<sub>4</sub>, NaOH, and KOH, were also screened for their effect on the reaction in H<sub>2</sub>O as solvent at 110 °C. A superior yield was obtained when K<sub>3</sub>PO<sub>4</sub> was used as the base (Table 1, entries 1-4). It is also noteworthy that, when this reaction was carried out with s-G or Fe<sub>3</sub>O<sub>4</sub>/s-G, we failed to isolate any coupled product (Table 1, entries 5 and 6).

Table 1 Screening of the reaction conditions<sup>a, a</sup>

Entry	Base	Time (h)	Yield (%) <sup>b</sup>
1	K <sub>2</sub> CO <sub>3</sub>	48h	27
2	NaOH	48h	50
3	KOH	48h	68
4	K <sub>3</sub> PO <sub>4</sub>	48h	95
5 <sup>c</sup>	K <sub>3</sub> PO <sub>4</sub>	48h	0
6 <sup>d</sup>	K <sub>3</sub> PO <sub>4</sub>	48h	0

<sup>a</sup>Phenyl iodide (1.0 mmol), Base (3.0 mmol), Au/Fe<sub>3</sub>O<sub>4</sub>/s-G (2 mol% of Au), 110°C, and H<sub>2</sub>O (2 ml). <sup>b</sup>GC yield, *n*-dodecane was used as an internal standard. <sup>c</sup> s-G (100 mg) <sup>d</sup> Fe<sub>3</sub>O<sub>4</sub>/s-G (100 mg)

With the optimized reaction conditions at hand, we next

managed to examine the scope and limitation of Ullmann coupling reaction with various types of aryl halides derivatives (Table 2). The aryl iodides bearing electron-donating and electron-withdrawing groups reacted well and gave good yields (Table 2, entries 1-4). The aryl iodide possessing electron-withdrawing group (*p*-COCH<sub>3</sub> and *p*-NO<sub>2</sub>) exhibited higher yield compared to an aryl iodide possessing electron-donating groups (*p*-OMe and *p*-Me) (Table 2, entries 2-4). The hindered 2-iodotoluene and 2-iodo-1,3,5-trimethylbenzene substrates converted to the corresponding homocoupling product with lower yield (Table 2, entries 6-7). Under the same reaction conditions the homocoupling of bromobenzene and aryl bromide bearing electron-donating and electron-withdrawing groups failed to form of homocoupled products (Table 2, entries 8-10).

Table 2. Au/Fe<sub>3</sub>O<sub>4</sub>/s-G nanocomposite catalyzed Ullmann coupling

Entry	R	X	Yield (%) <sup>a</sup>
1	H	I	95
2	4-OMe	I	84
3	4-Me	I	75
4	4-MeCO	I	98
5	4-NO <sub>2</sub>	I	91
6	2-Me	I	53
7	1,3,5-Trimethyl	I	36
8	H	Br	Trace.
9	4-Me	Br	Trace
10	4-MeCO	Br	Trace

<sup>a</sup> Isolated yields

Recently, Karimi presented a new strategy (double-separation technique) that includes easy separation of the catalyst by an external magnetic field as well as low solubility catalyst in organic solvents.<sup>39</sup> The presence of hydrophilic SO<sub>3</sub>H in the surface of magnetic nanocomposite provides a means of complete dispersion of the catalyst into the aqueous phase as far as the nanocomposite have no affinity to the organic phase. Considering this property, after the first use of the catalyst in the above mentioned Ullmann coupling reaction, the product was simply extracted with *n*-hexane while Au/Fe<sub>3</sub>O<sub>4</sub>/s-G nanocomposite remained in the aqueous phase (Fig. 5c). In the next stage, the aqueous phase containing Au/Fe<sub>3</sub>O<sub>4</sub>/s-G nanocomposite was recharged with phenyl iodide and K<sub>3</sub>PO<sub>4</sub><sup>40</sup> for the next run without any washing and purification of the catalyst. The results indicate that this simple separation method could be repeated for five consecutive runs and the recovered aqueous phase containing the Au/Fe<sub>3</sub>O<sub>4</sub>/s-G nanocomposite showed remarkably constant catalytic activity in all of 5 cycles (Table 3). Additionally, it was observed that the yield of the product gradually dropped with each reaction cycle. To verify whether any leaching occurs, the gold content in the used Au/Fe<sub>3</sub>O<sub>4</sub>/s-G nanocomposite (after 5 cycles) was analyzed by ICP-OES and it revealed the loss of about 5.4% of the initial amount of gold that was originally present in the fresh nanocomposite. Finally, the magnetic nanocomposite was easily and completely separated from the aqueous phase by an external magnetic field (Fig. 5b).

Table 3. Reusability of the Au/Fe<sub>3</sub>O<sub>4</sub>/s-G nanocomposite in the Ullmann coupling reaction of phenyl iodide<sup>a</sup>

Reaction cycle	1st	2nd	3rd	4th	5th
Yield <sup>b</sup> (%)	95	94	89	82	78

<sup>a</sup>Phenyl iodide (1.0 mmol), K<sub>3</sub>PO<sub>4</sub> (3.0 mmol), Au/Fe<sub>3</sub>O<sub>4</sub>/s-G (2.0 mol% of Au), 48 h and H<sub>2</sub>O (2 ml).

<sup>b</sup> GC yield, *n*-dodecane was used as an internal standard.

The heterogeneous nature of the catalysis was proved using a hot filtration test, atomic absorption spectroscopy (AAS) analysis and Hg<sup>0</sup>-poisoning experiment. To determine whether the catalyst is actually acted in a heterogeneous manner or whether it is merely a reservoir for more active soluble gold species, we performed a hot filtration test in the Ullmann coupling reaction of phenyl iodide after ~50% of the coupling reaction was completed. The hot filtrates were then transferred to another flask containing K<sub>3</sub>PO<sub>4</sub> (3 equiv.) in H<sub>2</sub>O (2 ml) at 110 °C. Upon further heating of catalyst-free solution for 48 h, no considerable progress (~9% by GC analysis) was observed. Moreover, applying AAS to the same reaction solution at the midpoint of completion indicated that no significant quantities of gold are left to the reaction liquors during the process. To determine whether the catalyst is heterogeneous or homogeneous,<sup>41</sup> a mercury poisoning experiment was performed. With standard reaction conditions for the Ullmann homo-coupling reaction, an experiment with Au/Fe<sub>3</sub>O<sub>4</sub>/s-G nanocomposite was started as described above: phenyl iodide (1.0 mmol), K<sub>3</sub>PO<sub>4</sub> (3 mmol), and Au/Fe<sub>3</sub>O<sub>4</sub>/s-G (2.0 mol% of Au) in H<sub>2</sub>O (2 mL) were reacted in a stainless-steel bomb. After about 24 h, the reaction was stopped, and the excess of Hg<sup>0</sup> (60 mmol) was added, and the reaction was then restarted. The yield for 24 h was 46% and for an additional 24 h after the addition of mercury it was 47%. This result clearly demonstrates the heterogeneous nature of the catalyst.

Table 4, compares efficiency of Au/Fe<sub>3</sub>O<sub>4</sub>/s-G nanocomposite (size of Au NPs, reaction conditions, time, and yield) with efficiency of other reported heterogeneous gold nanoparticles catalysts in Ullmann homocoupling reaction of phenyl iodide. These result indicated that the size of Au NPs does not change the reactivity in Ullmann homocoupling.

Table 4. Comparison of efficiency of various gold nanoparticle catalysts in Ullmann homocoupling reaction of phenyl iodide

Catalyst	Size of Au NPs	Condition	Yield	Time	Ref.
Au/Fe <sub>3</sub> O <sub>4</sub> /s-G	20-35 nm	K <sub>3</sub> PO <sub>4</sub> , H <sub>2</sub> O, 100 °C	95 %	48 h	This work
Au NPs-RGO	10-20 nm	K <sub>3</sub> PO <sub>4</sub> , NMP, 100 °C	97 %	6 h	24
Au@PMO	3-15 nm	K <sub>3</sub> PO <sub>4</sub> , NMP, 100 °C	95 %	16 h	14
Au NP	1 nm	H <sub>2</sub> O/TBAOH, glucose, 100 °C	98 %	7 h	25
Au <sub>25</sub> (SR) <sub>18</sub> /CeO <sub>2</sub>	1.3 nm	K <sub>2</sub> CO <sub>3</sub> , DMF, 130 °C	99.8 %	48 h	22
NAP-Mg-Au	5-7 nm	K <sub>2</sub> CO <sub>3</sub> DMF, 140 °C	92 %	48 h	23

## Conclusions

In conclusion, we demonstrated that Au/Fe<sub>3</sub>O<sub>4</sub>/s-G nanocomposite as a new highly water-dispersible/magnetically

separable semi heterogeneous for catalysis of organic reaction in aqueous medium. This nanocomposite is highly active catalyst for Ullmann coupling of aryl iodides in water. The catalyst exhibits extremely low solubility in organic solvents, the recovered aqueous phase containing the catalyst can be easily recycled using an external magnet and reused at least five times without loss of catalytic activity. Leaching tests such as hot filtration test and the AAS analysis indicate that the catalytic reaction is mainly heterogeneous in nature.

## Notes and references

<sup>a</sup> Faculty of Chemistry, Shahid Beheshti University, Tehran, Islamic Republic of Iran. Fax: +98 21 22431661; Tel: +98 21 29903255; E-mail: m-dabiri@sbu.ac.ir

<sup>b</sup> Department of Marine Biology, Faculty of Biological Sciences, Shahid Beheshti University, G. C., Evin, Tehran, Iran

† Electronic Supplementary Information (ESI) available: [details of any supplementary information available should be included here]. See DOI: 10.1039/b000000x/

- Z. Li, C. Brouwer and C. He, *Chem. Rev.*, 2008, **108**, 3239; R. Skouta and C.-J. Li *Tetrahedron*, 2008, **64**, 4917; I. Nakamura and Y. Yamamoto, *Chem. Rev.*, 2004, **104**, 2127; C.-J. Li, *Acc. Chem. Res.*, 2002, **35**, 533; Jia, C.; Kitamura, T.; Fujiwara, Y. *Acc. Chem. Res.*, 2001, **34**, 633; G. S. Fonseca, A. P. Umpierre, P. F. P. Fichtner, S. R. Teixeira and J. Dupont *Chem. Eur. J.*, 2003, **9**, 3263.
- A. Schatz, O. Reiser and W. J. Stark, *Chem.-Eur. J.*, 2010, **16**, 8950; E. Antolini, *Appl. Catal., A*, 2009, **88**, 1; L. Zhou, C. Gao and W. Xu, *Langmuir*, 2010, **26**, 11217; X. Tan, W. Deng, M. Liu, Q. Zhang and Y. Wang, *Chem. Commun.*, 2009, 7179; T. Mitsudome, A. Noujima, T. Mizugaki, K. Jitsukawa and K. Kaneda, *Adv. Synth. Catal.*, 2009, **351**, 1890; M. S. Chen and D. W. Goodman, *Science*, 2004, **306**, 252.
- K. K. R. Datta, B. V. S. Reddy, K. Ariga and A. Vinu, *Angew. Chem. Int. Ed.*, 2010, **49**, 5961; C. Marsden, E. Taarning, D. Hansen, L. Johansen, S. K. Klitgaard, K. Egeblad and C. H. Christensen, *Green Chem.*, 2008, **10**, 168; B. Zhu, M. Lazar, B.G. Trewyn and R.J. Angelici, *J. Catal.*, 2008, **260**, 1; Y. Taia, J. Murakamia, K. Tajirib, F. Ohashib, M. Datéc and S. Tsubotac, *Appl. Catal. A*, 2004, **268**, 183; P. Claus, *Appl. Catal. A*, 2005, **291**, 222; P. Garcia, M. Malacria, C. Aubert, V. Gandon and L. Fensterbank, *ChemCatChem*, 2010, **2**, 493; N. Zhang, H. Qiu, Y. Liu, W. Wang, Y. Li, X. Wang and J. Gao, *J. Mater. Chem.*, 2011, **21**, 11080; G. Li, D.-e. Jiang, C. Liu, C. Yu and R. Jin, *J. Catal.*, 2013, **306**, 177; J. Mielby, S. Kegnæs and P. Fristrup, *ChemCatChem*, 2012, **4**, 1037-1047.
- A. Corma and H. Garcia, *Chem. Soc. Rev.*, 2008, **37**, 2096.
- S. Carretin, P. Concepción, A. Corma, J. M. López Nieto and V. F. Puentes, *Angew. Chem., Int. Ed.*, 2004, **43**, 2538.
- R. Resch, S. Meltzer, T. Vallant, H. Hoffmann, B. E. Koel, A. Madhukar, A. A.G. Requicha and P. Will, *Langmuir*, 2001, **17**, 5666; G. Rizza, Y. Ramjauny, T. Gacoin, L. Vieille and S. Henry *Phys. Rev. B*, 2007, **76**, 245414
- E. Bus, J.T. Miller and J. A. van Bokhoven, *J. Phys. Chem. B*, 2005, **109**, 14581; Y.-F. Han, Z. Zhong, K. Ramesh, F. Chen and L. Chen, *J. Phys. Chem. C*, 2007, **111**, 3163.
- A. Dawson and P.V. Kamat, *J. Phys. Chem. B*, 2001, **105**, 960; R. Zanella, S. Giorgio, C. R. Henry and C. Louis, *J. Phys. Chem. B*, 2002, **106**, 7634; X. Wang and R. A. Caruso, *J. Mater. Chem.*, 2011, **21**, 20.
- W. Fang, J. Chen, Q. Zhang, W. Deng and Y. Wang, *Chem. Eur. J.*, 2011, **17**, 1247.
- F. Z. Su, Y. M. Liu, L. C. Wang, Y. Cao, H. Y. He and K. N. Fan, *Angew. Chem.*, 2008, **120**, 340.
- H. Tsunoyama, H. Sakurai, Y. Negishi, and T. Tsukuda, *J. Am. Chem. Soc.*, 2005, 127, 9374.
- H. Miyamura, R. Matsubara, Y. Miyazaki and S. Kobayashi *Angew. Chem., Int. Ed.*, 2007, **46**, 4151.

- 13 S. Wang, Q. Zhao, H. Wei, J.-Q. Wang, M. Cho, H. S. Cho, O. Terasaki and Y. Wan, *J. Am. Chem. Soc.*, 2013, **135**, 11849.
- 14 B. Karimi and F. K. Esfahani, *Chem. Commun.*, 2011, **47**, 10452.
- 15 M. Pumera, *Chem. Soc. Rev.*, 2010, **39**, 4146; X. Huang, X. Qi, F. Boey and H. Zhang, *Chem. Soc. Rev.*, 2012, **41**, 666; J. Yao, Y. Sun, M. Yang and Y. Duan, *J. Mater. Chem.*, 2012, **22**, 14313
- 16 T. Zeng, X. Zhang, Y. Ma, H. Niu and Y. Cai, *J. Mater. Chem.*, 2012, **22**, 18658; S. Bai and X. Shen, *RSC Adv.*, 2012, **2**, 64.
- 17 X. Li, X. Wang, S. Song, D. Liu and H. Zhang, *Chem. Eur. J.*, 2012, **18**, 7601.
- 18 A. H. Latham and M. E. Williams, *Acc. Chem. Res.*, 2008, **41**, 411; N. A. Frey, S. Peng, K. Cheng and S. H. Sun, *Chem. Soc. Rev.*, 2009, **38**, 2532; A. G. Roca, R. Costo, A. F. Rebolledo, S. Veintemillas-Verdaguer, P. Tartaj, T. González-Carreño, M. P. Morales and C. J. Serna, *J. Phys. D: Appl. Phys.*, 2009, **42**, 224002; M. A. M. Gijjs, F. Lacharme and U. Lehmann, *Chem. Rev.*, 2010, **110**, 1518.; C. S. S. R. Kumar and F. Mohammad, *Adv. Drug Deliv. Rev.*, 2011, **63**, 789.
- 19 S. Guo, S. Dong and E. Wang, *Chem. Eur. J.*, 2009, **15**, 2416; S. Guo, S. Dong and E. Wang, *J. Phys. Chem. C*, 2008, **112**, 2389; S. Guo, J. Li and E. Wang, *Chem. Asian J.*, 2008, **3**, 1544.
- 20 Y. Si and E.T. Samulski, *Nano Lett.*, 2008, **8**, 1679; S.-J. Li, Y.-F. Shi, L. Liu, L.-X. Song, H. Pang and J.-M. Du, *Electrochim. Acta* 2012, **85**, 628.
- 21 J. Hassan, M. Sevignon, C. Gozzi, E. Schulz and M. Lemaire, *Chem. Rev.*, 2002, **102**, 1359; T. D. Nelson and R. D. Crouch, *Org. React.*, 2004, **63**, 265.
- 22 G. Li, C. Liu, Y. Lei and R. Jin, *Chem. Commun.*, 2012, **48**, 12005.
- 23 K. Layek H. Maheswaran and M. L. Kantam, *Catal. Sci. Technol.*, 2013, **3**, 1147
- 24 S. Kazemi Movahed, M. Fakharian, M. Dabiri and A. Bazgir, *RSC Adv.*, 2014, **4**, 5243.
- 25 A. Monopoli, P. Cotugno, G. Palazzo, N. Ditaranto, B. Mariano, N. Cioffi, F. Ciminale and A. Nacci, *Adv. Synth. Catal.*, 2012, **354**, 2777.
- 26 J. Hu, Y. Wang, M. Han, Y. Zhou, X. Jiang and P. Sun, *Catal. Sci. Technol.*, 2012, **2**, 2332.
- 27 Y. Li, X. Fan, J. Qi, J. Ji, S. Wang, G. Zhang and F. Zhang, *Mater. Res. Bull.* 2010, **45**, 1413.
- 28 A. Jorio, M. S. Dresselhaus, R. Saito, G. F. Dresselhaus, in *Raman Spectroscopy in Graphene Related Systems*; Wiley-VCH: Berlin, 2011.
- 29 X.Fu, F. Bei, X. Wang, S. O'Brien and J. R. Lombardi, *Nanoscale*, 2010, **2**, 1461.
- 30 J.-Z. Wang, C. Zhong, D. Wexler, N. H. Idris, Z.-X. Wang, L.-Q. Chen and H.-K. Liu, *Chem. Eur. J.*, 2011, **17**, 661.
- 31 G. Goncalves, P. A. A. P. Marques, C. M. Granadeiro, H. I. S. Nogueira, M. K. Singh and J. Gracio, *Chem. Mater.*, 2009, **21**, 4796; A. Champion, J. E. Ivanecky and C. M. Child, *J. Am. Chem. Soc.*, 1995, **117**, 11807; H. Ko, S. Singamaneni and V. V. Tsukruk, *Small*, 2008, **4**, 1576.
- 32 M. A. Tamor and W. C. Vassell, *J. Appl. Phys.* 1994, **76**, 3823; V. Dharuman, J. H. Hahn, K. Jayakumar and W. Teng, *Electrochim. Acta*, 2013, **114**, 590.
- 33 J. Ji, G. Zhang, H. Chen, Y. Li, G. Zhang, F. Zhang, and X. Fan, *J. Mater. Chem.*, 2011, **21**, 14498; G. Zhao, L. Jiang, Y. He, J. Li, H. Dong, X. Wang, and W. Hu, *Adv. Mater.*, 2011, **23**, 3959.
- 34 N. Sakmeche, S. Aeiyaich, J.-J. Aaron, M. Jouini, J. C. Lacroix, and P.-C. Lacaze, *Langmuir*, 1999, **15**, 2566; M. G. Han, and S. H. Foulger, *Small*, 2006, **2**, 1164.
- 35 Z.-S. Wu, S. Yang, Y. Sun, K. Parvez, X. Feng, and K. Müllen, *J. Am. Chem. Soc.* 2012, **134**, 9082; W. Wu, Q. He, H. Chen, J. Tang and L. Nie, *Nanotechnology*, 2007, **18**, 145609.
- 36 R. Leppelt, B. Schumacher, V. Plzak, M. Kinne and R. J. Behm, *J. Catal.*, 2006, **244**, 137; H. G. Boyen, G. Kastle, F. Weigl, B. Koslowski, C. Dietrich, P. Ziemann, J. P. Spatz, S. Riethmuller, C. Hartmann, M. Moller, G. Schmid, M. G. Garnier and P. Oelhafen, *Science*, 2002, **297**, 1533.
- 37 J. Popplewell, L. Sakhnini and J. Magn, *Magn. Mater.*, 1995, **142**, 72.
- 38 X. Yang, X. Zhang, Y. Ma, Y. Huang, Y. Wang and Y. Chen, *J. Mater. Chem.*, 2009, **19**, 2710; J. Su, M. Cao, L. Ren and C. Hu, *J. Phys. Chem. C*, 2011, **115**, 14469.
- 39 B. Karimi, F. Mansouri and H. Vali, *Green Chem.*, 2014, **16**, 2587.
- 40 The amount of base needed in each run was estimated by pH analysis of the recovered aqueous reaction phase.
- 41 K. H. Park and Y. K. Chung, *Adv. Synth. Catal.*, 2005, **347**, 854.